Presented at the 2006 AIAA Guidance, Navigation, and Control Conference, August 21-24, Keystone, CO.

Finite-Horizon Robust Integrated Guidance-Control of A Moving-Mass Actuated Kinetic Warhead

P. K. Menon[*] , S. S. Vaddi[†]
Optimal Synthesis Inc., Palo Alto, CA 94303

and

Ernest J. Ohlmeyer[‡]
Naval Surface Warfare Center, Dahlgren, VA 22448

A game-theoretic approach to the design of robust integrated guidance-control system for a moving-mass actuated kinetic warhead is presented. Feedback linearized form of the kinetic warhead dynamics and a high-order target model are used in the formulation. Nonlinear feedback solution to the robust finite-horizon target interception problem is derived using the recently developed multi-stepping algorithm. Due to its computational efficiency, the multi-stepping algorithm is suitable for real-time implementation. Interception of targets in the presence of modeling uncertainties is demonstrated in nonlinear engagement simulations.

I. Introduction

Integrated synthesis of missile guidance and control systems has been of significant interest in the recent literature[1-9]. These techniques have been shown[8] to enhance missile performance by exploiting the synergism between guidance and control (autopilot) subsystems. By establishing additional feedback paths in the flight control system, integrated design methods allow the designer to realize beneficial interactions between these subsystems. A brief discussion on the motivation for designing integrated guidance-control systems will be given in Section II.

The present research focuses on the design of robust integrated flight control systems for moving-mass actuated[5] kinetic warheads. Since these vehicles must intercept the targets within a specified time interval, the flight control task is a finite-horizon control problem. The present research has its basis in recent work[7] on fixed-interval integrated guidance-control systems, and an efficient numerical algorithm[10] for computing finite-interval optimal control. Although the robustness of fixed-interval guidance-control laws[7] has been verified in Monte-Carlo simulations, that research did not explicitly include the robustness requirements in the design process.

The finite-horizon integrated guidance-control problem is formulated here as a differential game[11] in which the nonlinear controller is made robust with respect to worst-case, bounded disturbances. The nonlinear dynamics of the kinetic warhead and the target are first transformed into a linear, time-invariant form using feedback linearization[12-14]. The differential game corresponding to the robust control problem is then formulated with respect to the feedback linearized dynamics. Note that the present formulation of the feedback linearized robust finite-interval control problem is closely related to some of the control problems discussed in Reference 15. Note that a robust control approach similar to the present formulation has been previously proposed[16] for the infinite-horizon nonlinear control problems. The system dynamics and the feedback linearization scheme will be discussed in Section III.

The Hamiltonian system derived from the necessary conditions for optimality[11] is solved using the multi-stepping algorithm. The formulation and solution of the finite-horizon robust integrated guidance-control system design will be discussed in Section IV. Target engagement results using the finite-horizon robust integrated guidance control law will be given in Section V. Conclusions from the present research are given in Section VI.

---

[*] Chief Scientist, 868 San Antonio Road. Associate Fellow, AIAA.
[†] Research Scientist, 868 San Antonio Road, Member AIAA.
[‡] Senior Guidance and Control Engineer, Code G23, 17320 Dahlgren Road, Associate Fellow AIAA.

II. Integrated Guidance-Control Systems

Traditional approach to missile guidance and control system design has been to neglect interactions between the guidance and control systems, and to treat individual subsystems separately. Missile dynamics is split into relative position dynamics and short period dynamics components. Relative position dynamics is used to synthesize the guidance law, while the short period dynamics is employed in the autopilot design to stabilize the airframe and to track guidance commands. Designs are generated for each subsystem and then assembled together. If the overall system performance is unsatisfactory, subsystems are re-designed to improve the system performance. Due to its iterative nature, this latter part of the design process can be highly time-consuming and expensive.

Figure 1 illustrates the differences between traditional flight control system and the integrated guidance-control system. In the conventional approach, the guidance law does not employ the missile body rates or sensed acceleration components to generate autopilot commands. As a result, in engagement scenarios requiring agile maneuvers, the guidance commands can sometimes exceed the autopilot performance limits. If the autopilot employs integral feedback loops for improved command tracking response, these guidance commands can drive the flight control system unstable. Additionally, since the autopilot does not use target relative missile position and velocity components for feedback, it cannot adjust its response to accommodate for agile target maneuvers that may occur towards the end of the engagement.

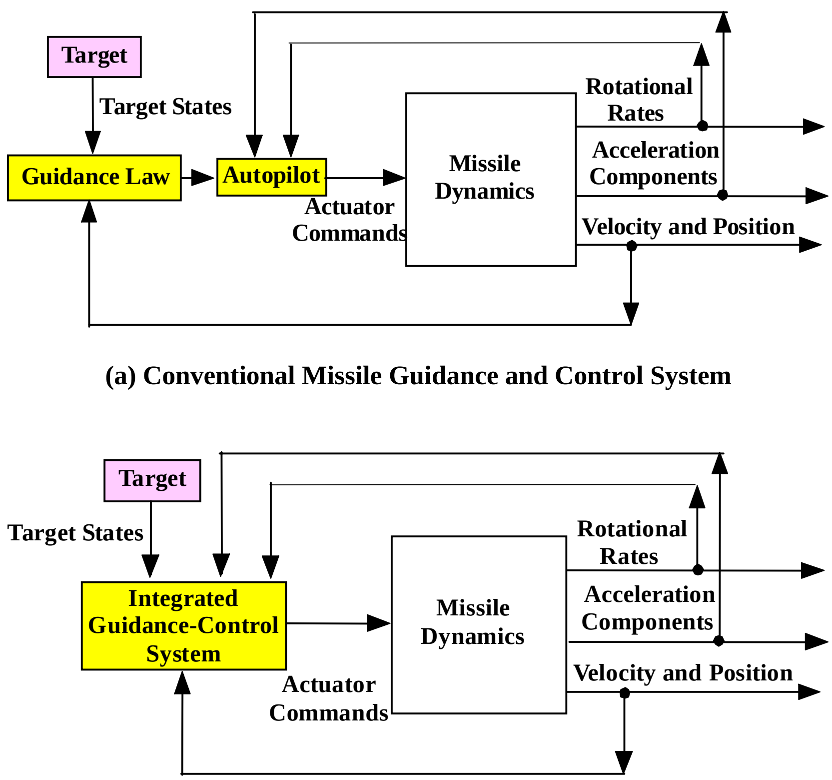

(a) Conventional Missile Guidance and Control System

(b) Integrated Guidance and Control System

Figure 1. Conventional and Integrated Guidance-Control Systems

Consequently, the traditional design approach requires the autopilot to have a small time constant when compared with the guidance system to assure the stability and performance of the overall flight control system. In fact, the autopilot time constant often dictates the achievable interception accuracy of missiles equipped with conventional flight control systems[17, 18]. While the autopilot time constant requirement can be easily met when the missile is far away from the target, it becomes increasingly difficult as the relative distance gets smaller. This is due to the fact that most guidance laws are functions of time-to-go, which make their guidance systems faster as the missile gets close to the target. In fact, it has been shown that conventional flight control systems can sometimes become unstable as the missile approaches the target[19].

On the other hand, in the integrated approach, the guidance and control functions are realized using all the available measurements. This fact makes the system is less likely to encounter saturation and stability problems.

Moreover, integrated design approach eliminates the iterative steps required to ensure the compatibility between the speed of response of the guidance and autopilot systems.

While there are definite operational advantages in employing integrated guidance-control systems, their design is complicated. This is due to the fact that the increased dimension of the nonlinear control problem makes it awkward to apply conventional gain-scheduling design methodology. These high-order designs may require gain scheduling not only with respect to the airframe performance variables, but also with respect to the engagement geometry. Although nonlinear control system design techniques can make these problems more tractable, symbolic manipulations required for their development can be formidable. Recent advancements in computer-aided nonlinear control system design technology[20, 21] offer more direct approaches for integrated system design, and avoid the need for any symbolic manipulations. The following section will discuss the kinetic warhead dynamics and the feedback linearization methodology.

III. Moving-Mass Actuated Kinetic Warhead and Feedback Linearization

The dynamics and control of a moving-mass actuated kinetic warhead was discussed in Reference 5. As illustrated in Figure 2, vehicle control is achieved by moving the actuating masses to alter the center of mass relative to the external forces. For instance, if the rocket motor thrust is aligned with the vehicle longitudinal body axis containing the nominal center of mass shown in Figure 2, moving the center of mass off the body centerline will result in moments about the pitch - yaw axes. Additionally, roll moments will be generated if the thrust or drag has an angular misalignment with respect to the longitudinal axis, or if the vehicle is subject to an aerodynamic lift force. The moving-mass control concept has been shown to be effective[5] for controlling the kinetic warhead equally well in space when the KW is thrusting, or in the atmosphere, when the vehicle experiences aerodynamic forces.

While the design of flight control systems using moving-mass actuation appears to be conceptually straightforward, difficulties arise due to the highly coupled and nonlinear nature of the system dynamics. This is partly due to the fact that in addition to causing changes in the vehicle center of mass, the moving-mass control system will exert inertial forces on the airframe. Moreover, the moving-masses will change the instantaneous moments of inertia of the flight vehicle, which will then contribute to changes in its dynamic response. The kinetic warhead flight control system designs must deliver the desired interception accuracy while accommodating these dynamic effects. Reference 5 showed the feasibility of designing nonlinear flight control systems for moving-mass actuated kinetic warheads to meet the accuracy requirements in both exo-atmospheric and atmospheric target interception scenarios. An infinite-horizon integrated guidance-control system regulating the pitch and yaw line-of-sight rates to achieve target interception was discussed that work.

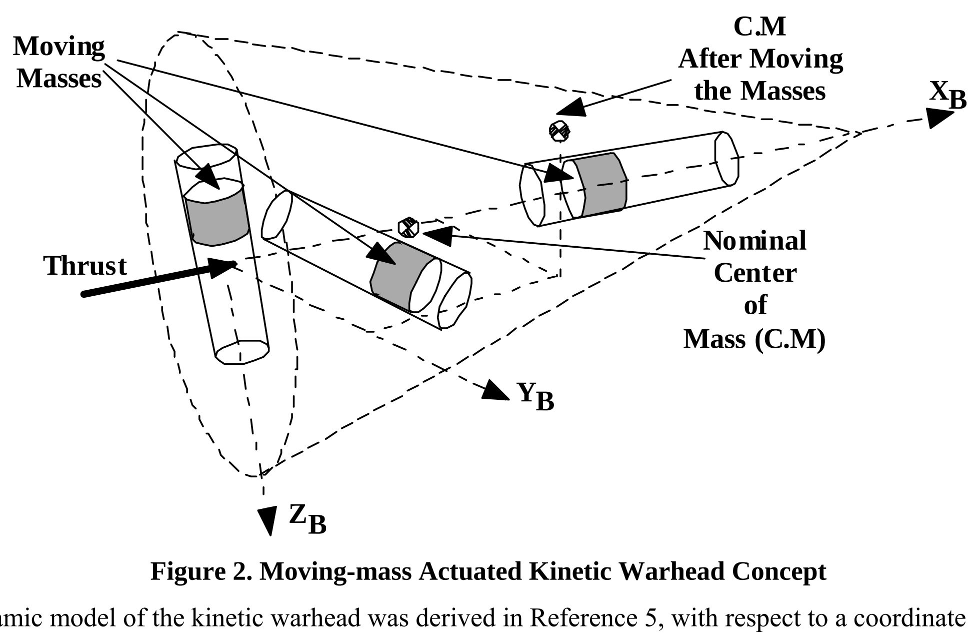

Figure 2. Moving-mass Actuated Kinetic Warhead Concept

The dynamic model of the kinetic warhead was derived in Reference 5, with respect to a coordinate system given in Figure 3. Starting from an initial position relative to the target, the interception occurs when the components of the relative position vector between the KW and the target Δ_x, Δ_y, Δ_z goes to zero. Since the relative position component Δ_x is not generally a controlled variable, the dynamics of the other two position components are used in guidance law derivation. This inertial frame for defining the relative position components is termed as the line-of-sight frame, and is chosen such its x-axis coincides with the line of sight vector at the initial time.

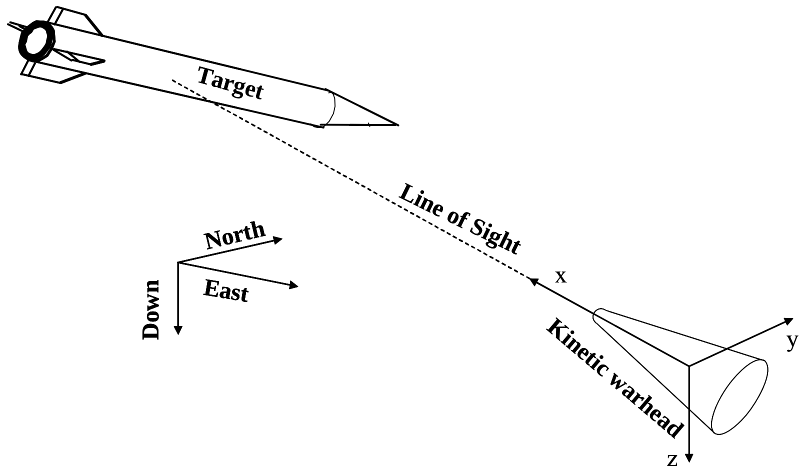

Figure 3. Kinetic Warhead and Target Engagement Scenario

The control mechanism can be illustrated through the following flow of the control variables through the system states.

$$\begin{aligned} &\delta_{yc} \to u_y \to \dot{\delta}_y \to \delta_y \to r \to \chi \to \dot{\Delta}_y \to \Delta_y \\ &\delta_{zc} \to u_z \to \dot{\delta}_z \to \delta_z \to q \to \theta \to \dot{\Delta}_z \to \Delta_z \end{aligned} \quad (1)$$

In the foregoing symbolic representation, the variable δ_{yc} is moving-mass position command to the y actuator and δ_{zc} is the position command to the moving-mass position command to the z actuator. The variables u_y, u_z are the forces applied by the linear actuators moving the masses, and $\delta_y, \dot{\delta}_y, \delta_z, \dot{\delta}_z$ are the position and rates of the moving masses. Kinetic warhead body rates are given by the variables q and r; and θ, χ are the pitch and yaw attitudes. Finally, the variables $\dot{\Delta}_y, \dot{\Delta}_z$ are the components of the relative velocity vector in the line-of-sight frame.

The expression (1) states that that the commands to the moving-mass actuators cause actuator forces to be applied on the masses, which in turn cause them to develop rates and consequently displacements. These displacements cause center of mass movement, creating control moments from external forces, thereby causing pitch and yaw body rates. These body rates change the kinetic warhead attitudes, producing changes in the direction of flight.

Present research assumes proportional plus derivative servos for the moving-mass actuators, and contain feed-forward compensation for the kinetic warhead lateral acceleration. The moving-mass servo control laws are of the form:

$$u_y = k_p(\delta_{yc} - \delta_y) - k_v\dot{\delta}_y + m_y a_y, \quad u_z = k_p(\delta_{zc} - \delta_z) - k_v\dot{\delta}_z + m_z a_z \quad (2)$$

Here, k_p and k_v are the position servo gains, δ_y and δ_z are the actual positions of the moving masses, a_y and a_z are the acceleration components along the body-frame y and z axes, m_y and m_z are the moving-masses along the y and z body axes.

Starting from the control flow definitions given in equation (1), and a numerical simulation model of the kinetic warhead, the software discussed in Reference 20 can construct feedback linearized form of the system dynamics. The numerically feedback linearized system dynamics can then be used for control law design. A double integrator target model, falling under the action of gravity is assumed in the present work. Relative position dynamics are given by:

$$\Delta_y^{(2)} = \bar{a}_{ty} - \bar{a}_{ky}, \qquad \Delta_z^{(2)} = \bar{a}_{tz} - \bar{a}_{kz} \quad (3)$$

The target acceleration components $\bar{a}_{ty}, \bar{a}_{tz}$ will be assumed to consist of known components and uncertainties $\Delta\bar{a}_{ty}, \Delta\bar{a}_{tz}$. The relative position dynamics including the target acceleration uncertainty is given by:

$$\Delta_y^{(2)} = \bar{a}_{ty} + \Delta\bar{a}_{ty} - \bar{a}_{ky}, \qquad \Delta_z^{(2)} = \bar{a}_{tz} + \Delta\bar{a}_{tz} - \bar{a}_{kz} \tag{4}$$

Since the feedback linearized dynamics of the kinetic warhead involves six differentiations of the relative position components, it will be assumed that the uncertainty in the target motion can be specified in terms of the fourth derivatives of $\Delta\bar{a}_{ty}, \Delta\bar{a}_{tz}$.

The feedback linearized dynamics of the kinetic warhead – target dynamics, including the target acceleration uncertainty is of the form:

$$\begin{bmatrix} \Delta_y^{(6)} \\ \Delta_z^{(6)} \end{bmatrix} = \begin{bmatrix} F_y \\ F_z \end{bmatrix} + \begin{bmatrix} G_{yy} & G_{yz} \\ G_{zy} & G_{zz} \end{bmatrix} \begin{bmatrix} u_y \\ u_z \end{bmatrix} + \begin{bmatrix} \Delta\bar{a}_{ty}^{(4)} \\ \Delta\bar{a}_{tz}^{(4)} \end{bmatrix} \tag{5}$$

The functions $F_y, F_z, G_{yy}, G_{yz}\ G_{zy}\ G_{zz}$ are state-dependent nonlinear functions. In order to facilitate the design of guidance-control laws, the first two terms on the right hand side of Equation 5 are replaced by pseudo inputs u_{py} and u_{pz}.

$$\begin{bmatrix} u_{py} \\ u_{pz} \end{bmatrix} = \begin{bmatrix} F_y \\ F_z \end{bmatrix} + \begin{bmatrix} G_{yy} & G_{yz} \\ G_{zy} & G_{zz} \end{bmatrix} \begin{bmatrix} u_y \\ u_z \end{bmatrix} \tag{6}$$

The fourth derivative of the uncertain target acceleration vector is treated as an unknown, bounded disturbance vector in the control law derivation.

$$\begin{bmatrix} w_y \\ w_z \end{bmatrix} = \begin{bmatrix} \Delta\bar{a}_{ty}^{(4)} \\ \Delta\bar{a}_{tz}^{(4)} \end{bmatrix} \tag{7}$$

The feedback linearized system dynamics in Brunovsky canonical form is given by:

$$\Delta_y^{(6)} = u_{py} + w_y, \qquad \Delta_z^{(6)} = u_{pz} + w_z \tag{8}$$

The superscripts within parenthesis indicate the order of time derivative. In all that follows, the state vectors corresponding to the feedback linearized dynamic system are denoted as:

$$Y = \begin{bmatrix} \Delta_y & \Delta_y^{(1)} & \Delta_y^{(2)} & \Delta_y^{(3)} & \Delta_y^{(4)} & \Delta_y^{(5)} \end{bmatrix} \quad Z = \begin{bmatrix} \Delta_z & \Delta_z^{(1)} & \Delta_z^{(2)} & \Delta_z^{(3)} & \Delta_z^{(4)} & \Delta_z^{(5)} \end{bmatrix}$$

IV. Robust Finite-Interval Integrated Guidance-Control Law

Consider the linear dynamical system:

$$\dot{X}(t) = A\,X + B\,U + \Gamma\,W \tag{9}$$

X is the n dimensional state vector, U is an m dimensional control vector and W represents an l dimensional unknown disturbance vector. The system matrices $A_{n\times n}$, $B_{n\times m}$ and $\Gamma_{n\times l}$ are assumed to be time invariant for the following development. Note that the algorithms described in the following can readily accommodate time varying dynamics. Since the disturbance vector is unknown, it will be assumed that it acts on the system in such a way as to maximize the performance objective the control system is attempting to minimize.

Consider the min-maximization of a quadratic performance index of the form:

$$\min_{u}\max_{w}\left\{\tfrac{1}{2}X_f^T S_f X_f + \tfrac{1}{2}\int_{to}^{tf}\left(X^T QX + U^T RU - \mu W^T W\right)d\tau\right\} \tag{10}$$

Here, $X_f = X(t_f)$ is the state vector at the final time t_f, and the lower limit of integration t_0 represents the current time t. Time-to-go is defined as: $t_f - t_o$. The negative sign in the term containing the unknown disturbance identifies it as the maximizer. Following the missile guidance literature, time-to-go will be computed in the following using the range and range rate as:

$$t_{2go} = -\frac{Instantaneous\ Range}{Instantaneous\ Range\ Rate} \tag{11}$$

S_f is a positive semi-definite terminal state-weighting matrix. Q is a positive semi-definite state-weighting matrix and R is a positive definite pseudo-control weighting matrix. The parameter μ is unspecified, and is determined through an iteration[22]. Starting from ∞, the value of μ is decreased until the differential game fails to yield a positive value of the cost function.

The necessary conditions for the optimality of the differential game formulated using the performance index (10) and the differential constraints (9) yield the optimal control law as:

$$U = -R^{-1}B^T\lambda \tag{12}$$

The corresponding worst-case disturbance is given by:

$$W = \frac{1}{\mu}\Gamma^T\lambda \tag{13}$$

The costate vector can be determined by solving the Hamiltonian System:

$$\begin{bmatrix}\dot{X}\\ \dot{\lambda}\end{bmatrix} = \begin{bmatrix} A & -\left(BR^{-1}B^T - \frac{1}{\mu}\Gamma\Gamma^T\right)\\ -Q & -A^T\end{bmatrix}\begin{bmatrix}X\\ \lambda\end{bmatrix}, \quad X(0) = X_0, \quad \lambda(t_f) = S_f X(t_f) \tag{14}$$

The symbolic solution to the linear dynamic system (14) is given by:

$$\begin{bmatrix}X(t_f)\\ \lambda(t_f)\end{bmatrix} = e^{M(t_f - t_0)}\begin{bmatrix}X_0\\ \lambda_0\end{bmatrix}, \text{ where } M \equiv \begin{bmatrix} A & -\left(BR^{-1}B^T - \frac{1}{\mu}\Gamma\Gamma^T\right)\\ -Q & -A^T\end{bmatrix} \tag{15}$$

The solution to the two-point boundary value problem in Equation (14) can be constructed from the above symbolic solution if the state transition matrix of the Hamiltonian system can be computed for the given time interval. However, computation of the state transition matrix over large time intervals will generally lead to numerical difficulties.

A numerical algorithm for solving linear two-point boundary value problems such as the Equation (14) was given in Reference 10. In that approach, termed the multi-stepping algorithm, the given time interval divided into smaller intervals improve the numerical condition of the state transition matrix, to derive the solution to the two-point boundary-value problem. The algorithm is based on the idea that for sufficiently small time intervals, the state transition matrix can be calculated for any linear system. For the sake of clarity in the discussions, the multi-stepping algorithm will be outlined in the following.

As a first step, divide the given time interval $[0\ t_f]$ into subintervals of equal length 't_l' such as $[0\ t_l]$, $[t_l\ 2t_l]$,…….$[(n-1)t_l\ \ t_f]$. Note that the algorithm can be readily modified to accommodate unequal subintervals. The length of the subinterval is chosen such that the state transition matrix is numerically computable over the interval. The state transition matrix for each of these intervals is:

$$N = e^{Mt_l} = e^{M(t_2 - t_1)} = e^{M(t_1 + t_l - t_1)} = e^{Mt_l} = e^{M(t_3 - t_2)} \ldots\ldots \qquad (16)$$

The multi-stepping algorithm employs the relationship between the algebraic relationship between the state and costate co-state vectors to solve for the unknown boundary conditions. For the two-point boundary-value problem (14), it can be shown[10] that the states and the costates can be related as:

$$\lambda_i = S_i\, X_i \text{, with} \quad S_{i-1} = [N_{22} - S_i N_{12}]^{-1}[S_i N_{11} - N_{21}], \quad S(t_f) = S_f \qquad (17)$$

The expression (17) uses the $n \times n$ submatrices of the subinterval state transition matrix:

$$N = \begin{bmatrix} N_{11} & N_{12} \\ N_{21} & N_{22} \end{bmatrix} \qquad (18)$$

Note that the matrix S_i is the solution to the differential Riccatti equation. The initial value of the costate can be found by carrying out the recursions in (17) to the initial time, $t=0$.

$$\lambda_0 = S_0 X_0 \qquad (19)$$

The initial value of the costate vector can then be used to determine the optimal control and the worst-case disturbance at the initial time as:

$$U(0) = -R^{-1} B^T \lambda(0), \quad W(0) = \frac{1}{\mu} \Gamma^T \lambda(0) \qquad (20)$$

At each time instant, the initial value of the optimal control can considered as the feedback control against the worst-case disturbance. This differential game solution is used in the following section to derive the robust integrated guidance-control law for target interception.

V. Robust Integrated Guidance-Control Law for Target Interception

The target interception problem is posed as two finite-horizon differential games in the vertical and horizontal planes. The feedbacl linearized dynamics naturally decouples the system dynamics in these planes. The performance indices employed are:

$$J_y = \min_{u_{py}} \max_{w_y} \left\{ \frac{1}{2} Y_f^T S_f Y_f + \int_0^{t_{2go}} \left(\frac{1}{2} Y^T Q Y + \frac{1}{2} R u_{py}^2 - \mu w_y^T w_y \right) \right\} \qquad (21)$$

$$J_z = \min_{u_{pz}} \max_{w_z} \left\{ \frac{1}{2} Z_f^T S_f Z_f + \int_0^{t_{2go}} \left(\frac{1}{2} Z^T Q Z + \frac{1}{2} R u_{pz}^2 - \mu w_z^T w_z \right) \right\} \qquad (22)$$

From Section II, the state vector has six elements in each plane, and each plane has a scalar control variable. For the present research, the unknown disturbances are assumed to be scalars. The control and state weighting matrices used for the present study are:

R = 1e-2, Q(3,3) = 10000; Q(4,4) = 100, $S_f(1,1)$ *=1e8*

Other components of the state weight matrices Q and S_f are assumed to be zero. The solution to this game is obtained using the multi-stepping algorithm using 20 subintervals. As stated in Section II, the time-to-go is computed as the ratio of the range and range rate. After several iterations the value of μ that will yield a positive solution to the game was found to be 100. Identical design parameters were used for both horizontal and vertical plane guidance laws.

Performance of the integrated guidance-control law is next evaluated in a simulation. The block diagram of the simulation is given in Figure 4. A free falling target dynamic model is implemented in the control law derivation. It should be noted that the disturbance acceleration is obtained by integrating the worst case disturbance four times.

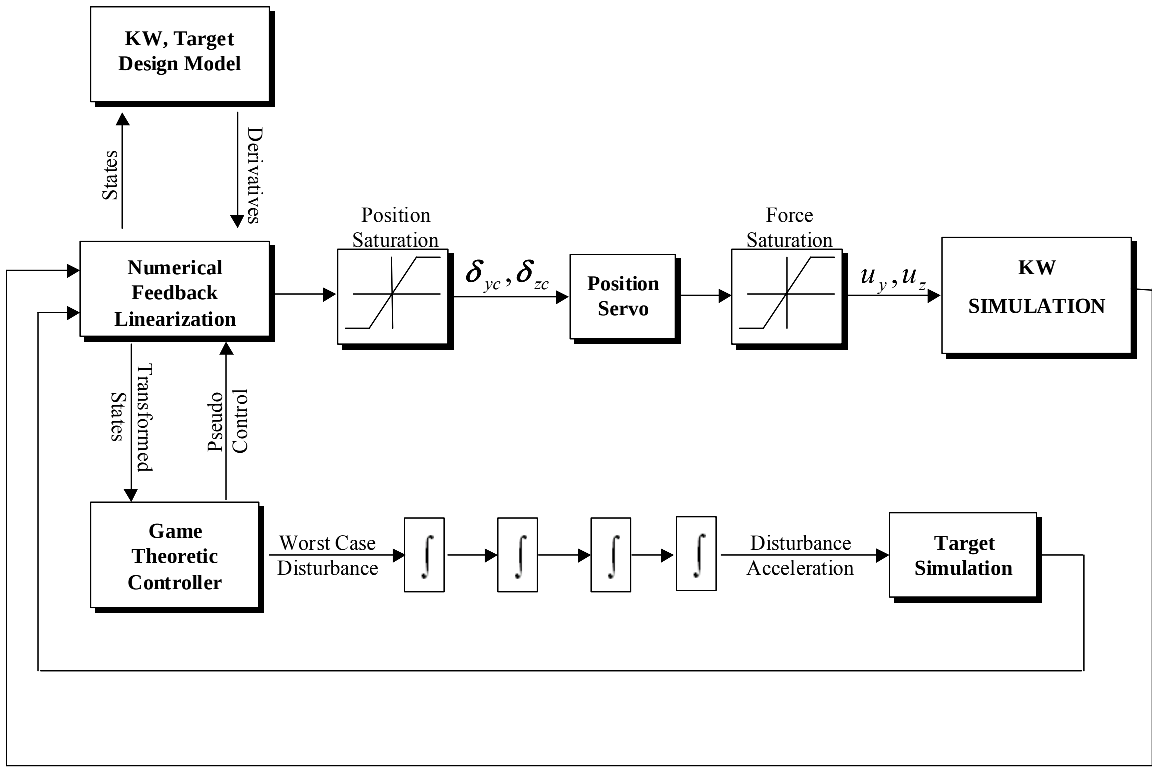

Figure 4. Block Diagram of the Robust Finite-Interval Guidance-Autopilot Simulation

For performance evaluations, the initial conditions on the target are chosen such that the target is descending from an altitude of 110,000ft and is 50,000ft away from the kinetic warhead in the North direction and 1,000ft away along the East direction. The kinetic warhead is ascending from an altitude of 60,000ft with a flight path angle of 45 degrees. Initial flight path angle of the target is -42degrees. Initial velocities of both the target and kinetic warhead are set to 6,000ft/s. Initial conditions on the positions and velocities of the moving masses, and body-rates are chosen to be zero. Initial attitudes of the kinetic warhead are chosen to result in zero angle of attack and angle of side-slip.

Figure 5 gives the target and the kinetic warhead trajectories in the 3-D space. The horizontal plane trajectories given in Figure 6 clearly shows the target attempting to maneuver away from the kinetic warhead towards the end of the interception. The worst-case disturbance acceleration components in the horizontal and the vertical planes, obtained by integrating the worst case disturbance four times are shown in Figure 7 and Figure 8. It may be observed that the worst-case disturbance appears to increase monotonically from its initial values. The time histories of the actuating masses during the engagement are given in Figure 9 and Figure 10. Both the commanded and the actual positions are shown in these figures. The moving mass positions are normalized with respect to the maximum displacement of the masses. The terminal miss distance for this engagement was 1.7ft.

Several other engagements have been simulated at the time of this writing. Performance comparisons previous formulations[5, 7, 10] are currently in progress.

Published by the American Institute of Aeronautics and Astronautics with Permission

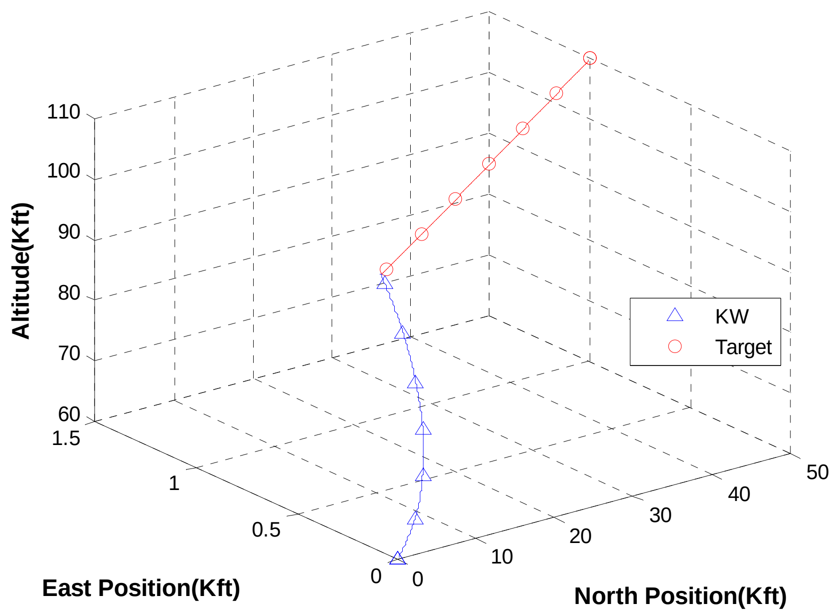

Figure 5. 3D Engagement Trajectories

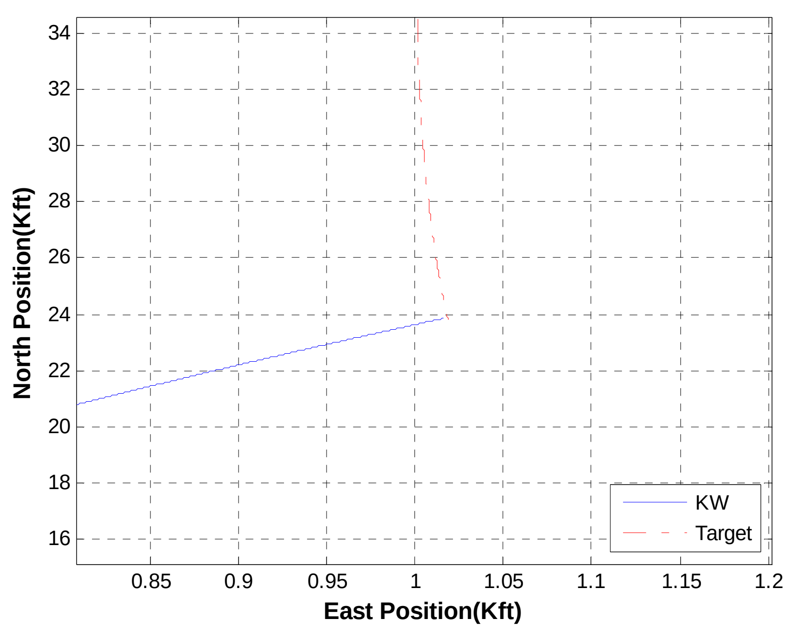

Figure 6. Horizontal Plane Trajectories

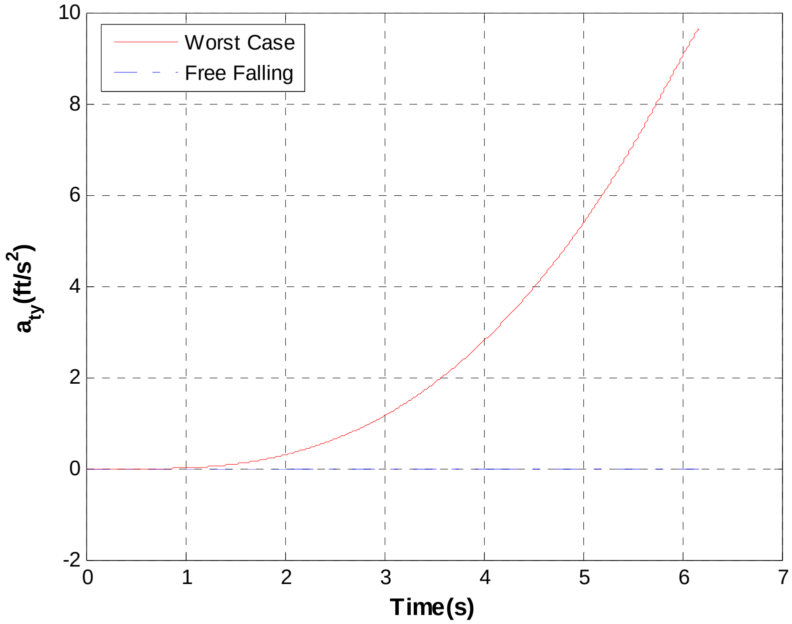

Figure 7. Free Falling and Worst Case Acceleration Components in the Horizontal Plane

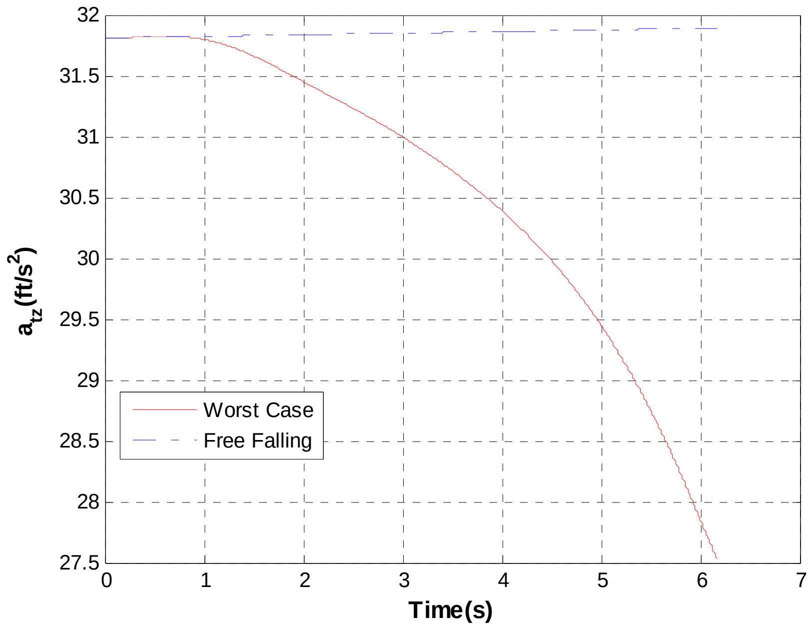

Figure 8. Free Falling and Worst Case Acceleration Components in the Vertical Plane

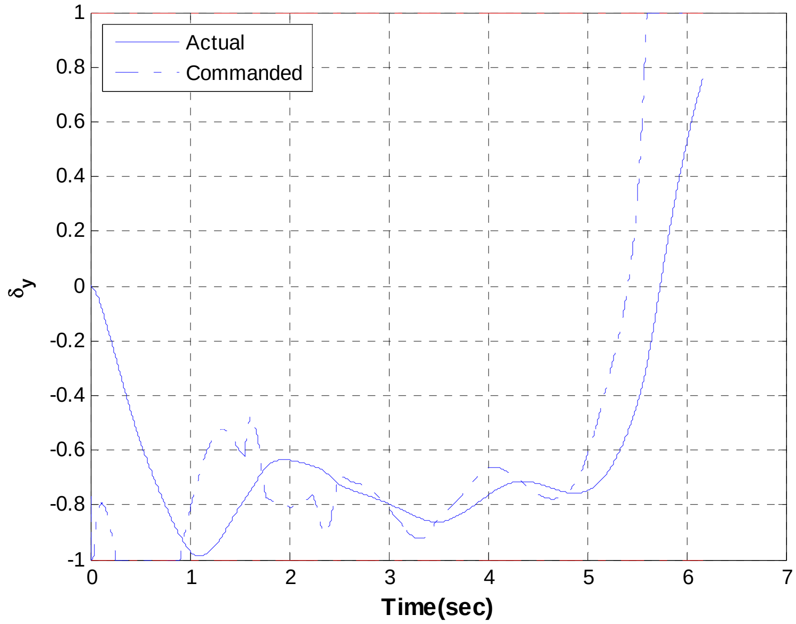

Figure 9. Commanded and Actual Positions of the Actuating Mass along in the Pitch Axis

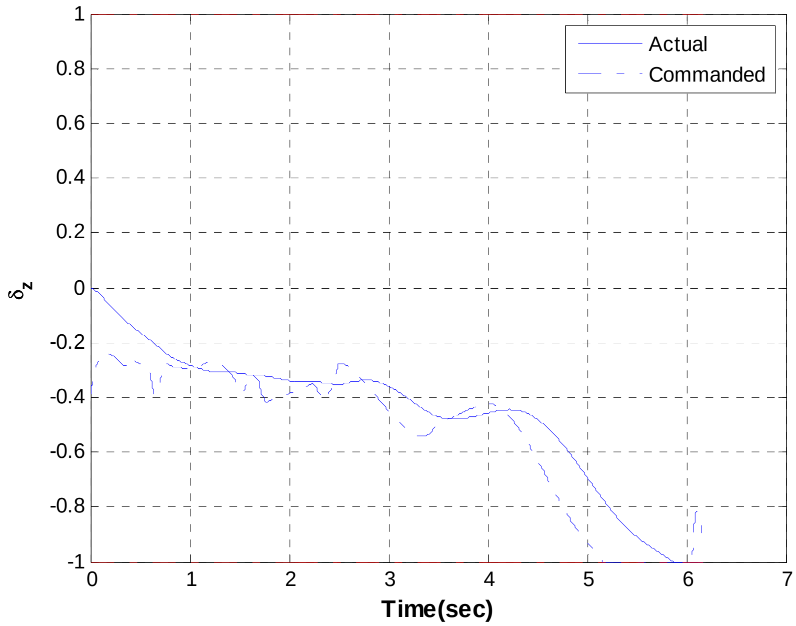

Figure 10. Commanded and Actual Positions of the Actuating Mass along the Yaw Axis

VI. Conclusions

This paper described the design of a finite-horizon, robust integrated guidance-control system for a moving-mass actuated kinetic warhead. The robust nonlinear control problem was formulated as a differential game using the feedback linearized dynamics of the kinetic warhead, and a free-falling target subjected to unknown disturbances. Feedback solution to the game-theoretic control problem was obtained using the multi-stepping algorithm. Results for a typical target engagement were given. Future research will compare the performance of the robust integrated guidance-control law with more conventional guidance-control system designs.

Acknowledgments

This research was supported under MDA Contract No. HQ0006-05-C-7261.

References

[1]Menon, P. K., Iragavarapu, V. R., and Ohlmeyer, E. J., "Integrated Design of Agile Missile Guidance and Control System", *AIAA Missile Sciences Conference*, November 17-19, 1998, Monterey, CA.

[2]Palumbo, N. F., and Jackson, T. D., "Integrated Missile Guidance and Control: A State Dependent Riccati Differential Equation Approach", *1999 IEEE International Conference on Control Applications*, August 22-27, Kohala Coast, Hawai'i.

[3]Menon, P. K., and Ohlmeyer, E. J., "Integrated Guidance-Control Systems for Fixed-Aim Warhead Missiles", *AIAA Missile Sciences Conference*, November 7-9, 2000, Monterey, CA.

[4]Menon, P. K. and Ohlmeyer, E. J., "Integrated Design of Agile Missile Guidance and Autopilot Systems", *IFAC* Journal of *Control Engineering Practice*, Vol. 9, 2001, pp. 1095-1106.

[5]Menon, P. K., Sweriduk, G. D., Ohlmeyer, E, J., and S. D. Malyevac, "Integrated Guidance and Control of Moving Mass Actuated Kinetic Warheads," *Journal of Guidance, Control, and Dynamics*, Vol. 27, No. 1, January-February 2004, pp. 118-126.

[6]Lin, C. F., Wang, Q., Speyer, J. L., Everes, J. H., and Cloutier, J. R., "Integrated Estimation, Guidance, and Control System Design Using Game Theoretic Approach", *Proceedings of the 1992 American Control Conference*, June-24-26, Chicago, IL, pp. 3220-3224.

[7]Menon, P. K., Sweriduk, G. D., and Ohlmeyer, E. J., "Optimal Fixed-Interval Integrated Guidance-Control Laws for Hit-to-Kill Missiles,"*2003 AIAA Guidance, Navigation and Control Conference*, Austin, Texas.

[8]Palumbo, N. F., Reardon, B. E., and Blauwkamp, R. A., "Integrated Guidance and Control of Homing Missiles," Johns Hopkins APL Technical Digest, Vol. 25, No. 2, 2004, pp. 121-139.

[9]Idan, M., Shima, T., and Golan, O., "Integrated Sliding Model Autopilot-Guidance for Dual Control Missiles," *2005 AIAA Guidance, Navigation and Control Conference*, Auguast 15 – 18, San Francisco, CA.

[10]Vaddi, S. S., Menon, P. K., Sweriduk, G. D., and Ohlmeyer, E. J., "Multi-Stepping Approach to Finite-Interval Missile Integrated Control," *Journal of Guidance, Control and Dynamics*, Vol. 29, No. 4, July-August 2006, pp. 1015-1018.

[11]Bryson, A. E., and Ho, Y. C., *Applied Optimal Control*, Hemisphere, New York, NY, 1975.

[12]Isidori, A., *Nonlinear Control Systems - An Introduction*, Springer-Verlag, New York, 1989.

[13]Slotine, J. J., and Li, W., *Applied Nonlinear Control*, Prentice-Hall, Englewood Cliffs, NJ, 1991.

[14]Marino, R., and Tomei, P., *Nonlinear Control Design*, Prentice-Hall, New York, NY, 1995.

[15]Bala Subrahmanyam, M., *Finite Horizon H∞ and Related Control Problems*, Birkhauser, Boston, MA, 1995.

[16]Menon, P. K., "Synthesis of Robust Autopilots using Differential Game Theory," 1991 *American Control Conference*, June 26 – 28, Boston, MA.

[17]Zarchan, P., *Tactical and Strategic Missile Guidance*, Progress in Astronautics and Aeronautics, Vol. 176, American Institute of Aeronautics and Astronautics, Reston, VA, 1997.

[18]Ohlmeyer, E. J., "Root-Mean-Square Miss Distance of Proportional Navigation Missile Against Sinusoidal Target," *Journal of Guidance, Control, and Dynamics*, Vol. 19, May-June, pp. 563-568.

[19]Guelman, M., "The Stability of Proportional Navigation Systems", *AIAA Guidance, Navigation and Control Conference*, August 20 –22, 1990, Portland, OR.

[20]Menon, P. K., Cheng, V. H. L., Lam, T. Crawford, L. S., Iragavarapu, V. R., and Sweriduk, G. D., *Nonlinear Synthesis Tools™ for Use with MATLAB®*, *Optimal Synthesis Inc.*, Palo Alto, CA, 2006.

[21]Menon, P. K. and Ohlmeyer, E. J., "Computer-Aided Synthesis of Nonlinear Autopilots for Missiles," *Journal of Nonlinear Studies*, Vol. 11, No. 2, 2004, pp. 173-198.

Presented at the 2006 AIAA Guidance, Navigation, and Control Conference, August 21-24, Keystone, CO.

[22]Bryson, A. E. and Carrier, "A Comparison of Control Synthesis using Differential Games (H-Infinity) and LQR," *AIAA Guidance, Navigation, and Control Conference*, 1989, Boston, MA.